

# Elementary Steps in the Formation of Hydrocarbons from Surface Methoxy Groups in HZSM-5 seen by Synchrotron Infrared Microspectroscopy

Ivalina B. Minova,<sup>a</sup> Santhosh K. Matam,<sup>b,c</sup> Alex Greenaway,<sup>b</sup> C. Richard A. Catlow,<sup>b,c,d</sup> Mark D. Frogley,<sup>e</sup> Gianfelice Cinque,<sup>e</sup> Paul A. Wright,<sup>a</sup> Russell F. Howe.<sup>f\*</sup>

<sup>a</sup> EastCHEM School of Chemistry, University of St Andrews, St Andrews KY16 9ST

<sup>b</sup> UK Catalysis Hub, Research Complex at Harwell, STFC Rutherford Appleton Laboratory, Didcot, Oxon OX11 0FA

<sup>c</sup> Cardiff Catalysis Institute, School of Chemistry, Cardiff University, Cardiff CF10 1AT

<sup>d</sup> Department of Chemistry, University College London, 20 Gower St., London WC1E 6BT

<sup>e</sup> Diamond Light Source, Harwell Science and Innovation Campus, Didcot, OX11 0DE

<sup>f</sup> Chemistry Department, University of Aberdeen, AB24 3UE

## Supporting Information

---

Synchrotron infrared microspectroscopy has identified with high temporal resolution (down to 0.25 s) the initial events occurring when methanol vapour is contacted with a crystal of zeolite HZSM-5. The first alkenes are generated directly from methoxy groups formed at the acid sites via their deprotonation. These alkenes can either desorb directly or oligomerise and cyclise to form dimethylcyclopentenyl cations. The oligomeric and dimethylcyclopentenyl cations are the first major components of the hydrocarbon pool that precede aromatic hydrocarbons and lead to indirect alkene formation. The technique observes these events in real time.

---

*Key Words:* synchrotron infrared microspectroscopy; ZSM-5; methanol-to-hydrocarbons; hydrocarbon pool; carbon-carbon bond formation

The methanol-to-hydrocarbon (MTH) process was first commercialised in the 1980s with an initial emphasis on gasoline production over a ZSM-5 zeolite catalyst.<sup>1</sup> More recent developments have emphasised alkene production from methanol, either over ZSM-5<sup>2</sup> or SAPO-34 zeolites.<sup>3,4</sup> The mechanisms of hydrocarbon formation over HZSM-5 and other zeolites have been widely investigated. Two recent reviews summarise the different theories which have been proposed.<sup>5,6</sup> It is now widely accepted that under steady state working conditions alkenes and aromatic hydrocarbons are produced from a 'hydrocarbon pool' within the zeolite pores, comprising a mixture of cyclic alkene and aromatic hydrocarbons from which reaction products are cracked and/or desorbed. It is less well understood how the hydrocarbon pool is formed in the first instance and in particular how the first carbon-carbon bonds are formed from a reactant which contains only carbon-oxygen bonds. The first step in carbon-carbon bond formation is generally agreed to involve reaction of methanol with the Brønsted acid hydroxyl groups in the zeolite to form surface methoxy groups and eliminate water. The surface methoxy groups are key intermediates in the subsequent catalysis. Ono

and Mori<sup>7</sup> first showed evidence for methoxy group formation in HZSM-5 from infrared spectroscopy using CD<sub>3</sub>OH. Early *operando* infrared spectroscopic measurements reported by Forester *et al.* showed that both methanol and dimethylether vapour contacting HZSM-5 at reaction temperatures generated surface methoxy groups which were active methylating agents.<sup>8,9</sup> Evidence for formation of methoxy groups even at room temperature has been presented recently.<sup>10,11</sup> NMR evidence for these active methoxy groups has also been reported. In particular, Wang *et al.*<sup>12</sup> used a stopped flow NMR technique to isolate methoxy groups and showed that they could methylate a range of different molecules (thus forming carbon-carbon bonds). These authors also demonstrated that in the absence of other reacting species the methoxy groups could generate alkenes directly.

Once methoxy groups are formed several different pathways to carbon-carbon bond formation have been suggested, with varying degrees of experimental support.<sup>5,6</sup> For example, methylation of dimethylether by methoxy groups to form the trimethyloxonium cation (which can undergo a subsequent

rearrangement to form methylethylether),<sup>13</sup> hydride abstraction from methanol by the methoxy groups to form methane and formaldehyde,<sup>14,15</sup> an equivalent pathway involving methoxymethyl cations<sup>16</sup> or the recently proposed carbonylation of methoxy groups by carbon monoxide (generated from methanol decomposition) to form methylacetate as the first carbon-carbon bond containing species.<sup>17,18</sup> Yamazaki *et al.* have presented infrared evidence for the formation of propene by direct reaction of surface methoxy groups with dimethylether over HZSM-5,<sup>19</sup> and two-dimensional NMR spectroscopy has revealed correlations between surface methoxy groups and adsorbed methanol in HSAPO-34, a smaller pore zeolite, suggestive also of direct reaction between the methoxy groups and methanol.<sup>20,21</sup>

Conventional spectroscopy of zeolite catalysts (transmission or diffuse reflectance infrared and NMR) inevitably report spectra integrated over many crystals in the sample. These macroscopic sampling techniques cannot respond quickly to rapid changes in local concentrations of reactants under *operando* conditions. The use of synchrotron infrared microspectroscopy to obtain high quality infrared spectra from large individual crystals of HZSM-5 catalysts was first reported by Stavitski *et al.*<sup>22</sup> This and subsequent work has exploited the *spatial* resolution of the technique down to 3-5  $\mu\text{m}$ .<sup>23,24</sup> We report here achieving high *temporal* resolution, facilitated by the enhanced brightness of a synchrotron source, to perform *operando* infrared microspectroscopy on a time scale as short as 0.25 s on individual crystals of HZSM-5. When coupled with simultaneous mass spectral (MS) analysis of desorbed products, the *operando* infrared microspectroscopy (OIMS) technique identifies the initial steps of formation of the hydrocarbon pool in HZSM-5.

An induction period in the formation of alkenes, when HZSM-5 is first exposed to methanol at reaction temperatures, is well known.<sup>1</sup> The measurements reported here on individual crystals show that the induction period does not arise from the conversion of methanol to dimethylether at 573 K but rather from a subsequent reaction step that involves the loss of the methoxy groups, regeneration of acid sites and the subsequent generation of oligomeric hydrocarbon. The oligomer containing carbon-carbon bonds is subsequently converted to a cyclic dimethylcyclopentenyl cation. These two species are the first components of the hydrocarbon pool.

Full details of the preparation and characterisation of large HZSM-5 crystals via a modified literature method, evaluation of their performance in a conventional catalytic microreactor, and the configuration of the infrared microspectroscopy experiment are given in the Supporting Information. Batches of crystals with different uniform size distributions were prepared and studied. Here are reported measurements on HZSM-5 crystals typically  $150 \times 60 \times 60 \mu\text{m}^3$  in size, using microscope apertures of  $15 \times 15 \mu\text{m}^2$ . The effects of crystal size will be reported in more detail elsewhere.<sup>25</sup>

Fig. 1 shows the reactivity of methanol over a HZSM-5 crystal at 573 K (spectra recorded at 2 s intervals with an 8  $\mu\text{L}$  pulse and at 0.25 s intervals with a 4  $\mu\text{L}$  pulses). Following injection of the 8  $\mu\text{L}$  pulse of methanol (Fig. 1a), the zeolite Brønsted  $\nu(\text{OH})$  band at  $3600 \text{ cm}^{-1}$  decreases within 60 s to 30% of its original intensity. The MS analysis of gases evolved from the Linkam cell (Fig. 1b) shows the formation of

dimethylether ( $m/z = 45$ ) within several seconds of methanol injection. Formation of dimethylether from methanol is the first step in the conversion of methanol to hydrocarbons.<sup>1</sup> Dimethylether hydrogen bonds to the Brønsted acid site. A full set of spectra is presented in Fig. S10 showing the characteristic  $\nu(\text{CH}_3)$  modes of hydrogen bonded dimethylether and the so-called ABC triplet of the strongly hydrogen bonded zeolite hydroxyl groups arising from Fermi resonance between the  $\nu(\text{OH})$  mode and the overtones of the corresponding  $\delta$  and  $\gamma$  deformation modes.<sup>26,27</sup> Dimethylether forms via the sequential dissociation of methanol at acid sites to form methoxy groups followed by methylation of a second methanol to form dimethylether.<sup>7-9,28</sup> In the spectra shown in Fig. S10 the characteristic infrared signature of surface methoxy groups in ZSM-5 in the  $\nu(\text{CH})$  region (bands at  $2980 \text{ cm}^{-1}$  and  $2870 \text{ cm}^{-1}$ , due to asymmetric and symmetric  $\text{CH}_3$  stretching modes, respectively<sup>7-9,28</sup>) is initially obscured by the overlapping bands of hydrogen-bonded dimethylether.

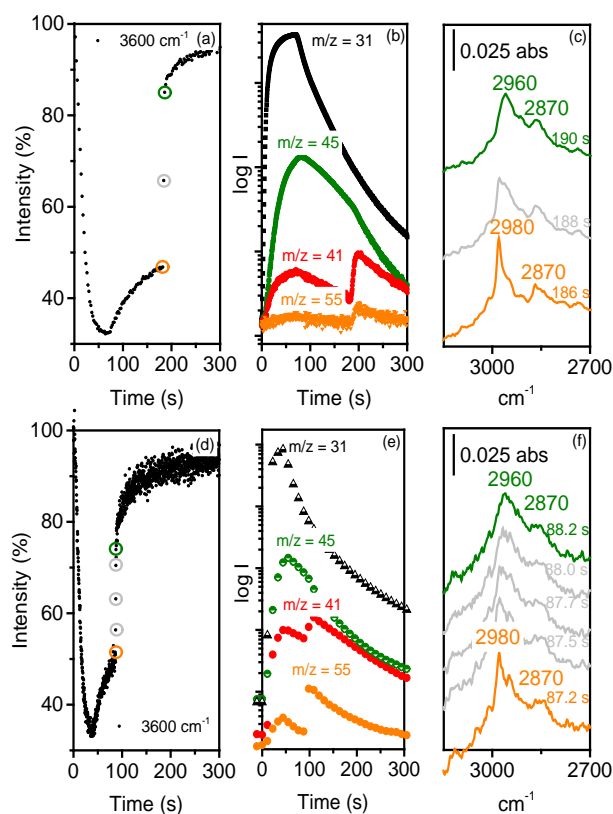


**Figure 1.** (a) Time course of the  $\nu(\text{OH})$   $3600 \text{ cm}^{-1}$  band intensity relative to an activated crystal recorded at 2 s intervals during the first 8  $\mu\text{L}$  methanol pulse injected into a  $\text{N}_2$  flow of  $100 \text{ mL min}^{-1}$  over an HZSM-5 crystal at 573 K; (b) MS traces recorded during this experiment.  $m/z = 31$  measures methanol,  $m/z = 45$  DME,  $m/z = 41$  propene (with a contribution from DME fragmentation),  $m/z = 55$  butene; (c) Evolution of the CH stretching region between 186 and 190 s; (d) The same experiment performed with 0.25 s time resolution during a 4  $\mu\text{L}$  methanol pulse over a crystal from the same batch at 573 K; (e) the corresponding MS traces and (f) evolution of the CH stretching region between 87.2 and 88.2 s after injection.

Fig. 1 shows that as the dimethylether is desorbed from the crystal (between 60 and 180 s after injection of an 8  $\mu\text{L}$  pulse of methanol), the  $\nu(\text{CH})$  bands of surface methoxy groups at  $2980\text{ cm}^{-1}$  and  $2870\text{ cm}^{-1}$  become visible (Fig. 1c orange trace). The loss of dimethylether corresponds to the gradual recovery of  $\sim 15\%$  of the zeolite  $\nu(\text{OH})$  band. Subsequent to the complete loss of dimethylether an abrupt change occurs 188 s after injection of methanol. In this particular experiment, within 4 s the zeolite  $\nu(\text{OH})$  band suddenly recovers to  $\sim 90\%$  of its original intensity (Fig. 1a). At the same time the  $\nu(\text{CH})$  bands of surface methoxy groups ( $2980$  and  $2870\text{ cm}^{-1}$ ) are completely converted to new  $\nu(\text{CH})$  bands at  $2960$  and  $2870\text{ cm}^{-1}$ , the latter broader than its predecessor (Fig. 1c green trace); and the MS (Fig. 1b) shows simultaneous evolution of propene ( $m/z = 41$ ) and butene ( $m/z = 55$ ). (Note that the initial  $m/z = 41$  peak at  $\sim 90$  s in Fig. 1(b) is due to fragmentation of dimethylether). To define more closely the time scale on which the abrupt spectral changes are occurring we repeated the experiment described above on a fresh crystal using a smaller methanol pulse ( $4\text{ }\mu\text{L}$ ) at higher time resolution of  $0.25\text{ s}$  (Fig. 1d, e and f). The induction time for alkene formation was reduced to  $\sim 90$  s for the  $4\text{ }\mu\text{L}$  injection (cf. 188 s for the  $8\text{ }\mu\text{L}$  injection experiment), nonetheless the changes occurring in the  $\nu(\text{CH})$  region were closely similar to those described above, and occur within  $0.5\text{ s}$ .

These spectral changes were reproduced when methanol was injected into crystals from different synthesis batches and when varying the selected region analysed within an individual crystal, although the length of the induction period varies with crystal size as well as the methanol pulse size.

Fig. 2 illustrates an experiment examining the reactivity of methanol- $d_3$  ( $\text{CD}_3\text{OH}$ ) over a HZSM-5 crystal at  $573\text{ K}$ . Similarly to the previous experiment, an initial decrease in  $\nu(\text{OH})$   $3600\text{ cm}^{-1}$  band intensity relative to the fresh crystal was seen due to hydrogen bonding of dimethylether and the formation of methoxy groups ( $\text{ZOCd}_3$ ) immediately after injection of methanol- $d_3$ . Following a slow recovery of  $\nu(\text{OH})$  intensity over the subsequent  $\sim 90$  s due to desorption of hydrogen bonded dimethylether, an abrupt loss of methoxy groups occurs at around  $110$  s after injection of  $\text{CD}_3\text{OH}$  (Fig. 2c), this coincides with the point of alkene formation and a rapid growth of a  $\nu(\text{OD})$  band at  $2650\text{ cm}^{-1}$ .

A ZOD band can only arise from CD bond breaking. A weak band appears at  $2750\text{ cm}^{-1}$  at the same time as the CD bond breaks which is assigned to the  $\nu(\text{OD})$  counterpart of the silanol groups in the parent zeolite associated with defects in the crystal).<sup>28</sup>

In the effluent gas phase Fig. 2b, dimethylether- $d_6$  is the first product detected ( $m/z = 50$  with contributions at  $m/z = 48$  from fragmentation), but the growth of the  $\nu(\text{OD})$  bands correlates exactly with the MS detection of propene- $d_6$  ( $m/z = 48$ ) and propene- $d_5$  ( $m/z = 47$ ). (The earlier  $m/z = 47$  peak coincident with dimethylether is barely above baseline and may arise from a methanol- $d_2$  impurity as shown in Fig. S11).

Spectra in the  $\nu(\text{CD})$  region are more complex than their  $\nu(\text{CH})$  counterparts, due to overlap of overtones of CD bending modes,<sup>30</sup> and the frequency differences between species are less in the lower frequency range, so that it is not possible to clearly differentiate between loss of methoxy groups ( $\text{CD}_3$ ) and of residual dimethylether- $d_6$ . However, the formation of

zeolite OD groups can only occur through C-D bond breaking, and this correlates closely with propene formation (early static infrared experiments by Ono and Mori also report CD bond breakage during propene formation<sup>7</sup>). We deduce a reaction step represented formally as  $\text{ZOCd}_3 \rightarrow \text{ZOD} + \text{CD}_2$ , i.e. the methoxy groups react further as carbene-like species to generate alkenes rather than as  $\text{CD}_3$  cations.<sup>19,28,31</sup> The detection by MS of propene- $d_5$  also shows that further exchange subsequently occurs with zeolite OH groups, including the silanol groups (as also seen by the change in  $\nu(\text{OH})$  intensity at this point).

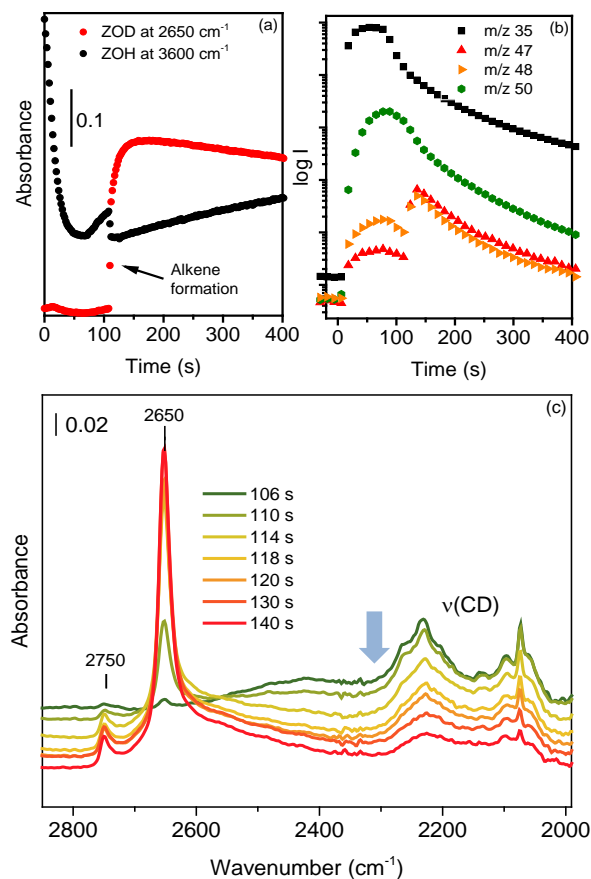


**Figure 2.** (a) Intensities of  $\nu(\text{OH})$  and  $\nu(\text{OD})$  bands following injection of  $8\text{ }\mu\text{L}$   $\text{CD}_3\text{OH}$  over a ZSM-5 crystal at  $573\text{ K}$ . (b) MS analysis of evolved gases.  $m/z = 35$  measures  $\text{CD}_3\text{OH}$ ,  $m/z = 50$  measures  $\text{CD}_3\text{OCD}_3$ ,  $m/z = 48$  measures propene- $d_6$  (with a contribution from fragmentation of  $\text{CD}_3\text{OCD}_3$ ),  $m/z = 47$  measures propene- $d_5$ . (c) corresponding changes in the  $\nu(\text{CD})$  and  $\nu(\text{OD})$  regions between 106 and 140 s after injection (every second spectrum plotted for clarity).

Once formed, alkenes can readily oligomerise in HZSM-5 and other acid zeolites at room temperature.<sup>32</sup> Propene forms an oligomer in HZSM-5 which has cationic character but which can be represented as  $\text{ZO-CH}(\text{CH}_3)\text{-(CH}_2\text{CH}(\text{CH}_3))_n\text{-CH}_2\text{-CH}(\text{CH}_3)_2$ , i.e. an alkoxide species replacing the acidic hydroxyl group.<sup>33,34</sup> The adsorbed species (characterised by infrared bands at  $2960$  and  $2870\text{ cm}^{-1}$  in the green trace of Fig. 1c) is identified as an oligomeric hydrocarbon cation that is generated at the same time as loss of surface methoxy spe-

cies, regeneration of Brønsted acid sites and the generation of alkenes.

This assignment of bands to an oligomer is based on spectra obtained in a parallel experiment, when a pulse of propene was injected into N<sub>2</sub> flowing over a fresh HZSM-5 crystal at 523 K: Fig. 3 shows selected spectra recorded at 2 s intervals. There is a striking similarity between the growing bands at 2960 cm<sup>-1</sup> and 2870 cm<sup>-1</sup> during the propene-pulse experiment (Fig. 3a), and the ν(CH) profile generated after alkenes are first formed during the methanol-pulse experiments (green traces in Figs. 1c and f), albeit at lower intensity and less well resolved in the case of methanol.

The intensities of the oligomer bands at 2960 cm<sup>-1</sup> (CH<sub>3</sub> asymmetric stretching mode) and 2870 cm<sup>-1</sup> (CH<sub>3</sub> and CH<sub>2</sub> symmetric stretching modes) decay with time and this correlates well with the MS trace of butene (m/z = 55) evolved during the propene pulse. A secondary peak can also be seen in the m/z = 41 trace due to propene. These correlations suggest that butene and secondary propene are formed by cracking and desorption of the oligomer.

As oligomer is lost, the spectrum evolves further. In particular, bands at 1510 and 1460 cm<sup>-1</sup> grow in intensity, then remain constant. These bands and others at 3120 and 2910 cm<sup>-1</sup>, which are evident in Fig. 3a after the oligomer species has declined, are considered further below. Similar spectral changes were seen when ethene was injected into a fresh crystal (See Fig. S13). Blank experiments showed a negligible contribution to the spectra from gas phase alkenes in the cell.

The question then arising is how the oligomer is formed in the first place. Is the oligomer formed directly from methoxy groups (2980, 2870 cm<sup>-1</sup>) and then cracked to form the alkenes, or are the alkenes detected by MS (m/z = 41 and 55) formed directly from methoxy groups and then go on to oligomerize?

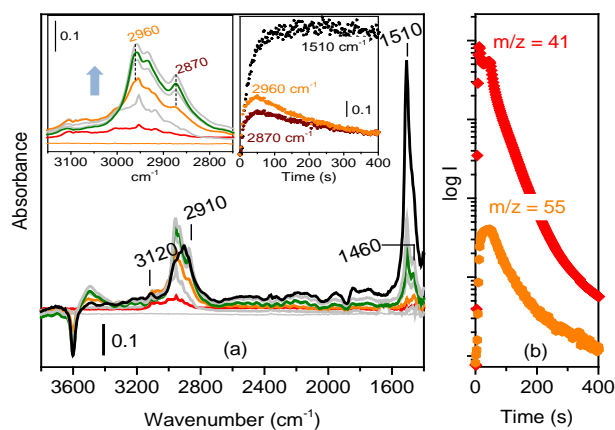


**Figure 3.** (a) Difference FTIR spectra recorded at 2 s intervals (first 6 scans shown) following a 2 mL propene pulse into a N<sub>2</sub> flow over an HZSM-5 crystal at 523 K. The overlaid black curve is the final spectrum in the series at 400 s after injection of propene. Insets show expansion of CH region and a plot of intensity of 2960, 2870 and 1510 cm<sup>-1</sup> bands versus time; (b) mass spectrometer traces following injection of propene at 523 K (m/z = 41 measures propene, and m/z = 55 butene).

To answer this question a temperature jump methanol-pulse experiment was performed. Fig. 4 describes the reactivity of surface methoxy groups, which were generated by injecting two successive pulses of methanol over an HZSM-5 crystal at 523 K and then holding the sample at this temperature in flowing nitrogen until the hydrogen bonded dimethylether was completely lost, so that the spectrum showed the characteristic fingerprint of methoxy groups (Fig. 4c). The OH intensity at this point (~ 70 % of the original) suggests that ~ 30% of the OH groups have formed methoxy groups. Note that in this experiment no residual bands of adsorbed dimethylether remain at this point. Then the temperature was raised by 5 K and the spectrum monitored versus time. After a further delay, OH intensity suddenly recovered to ~ 90% of that in the fresh crystal, and a burst of propene and butene was detected in the mass spectrum. No oligomer species were detected at this temperature (528 K), which suggests that the alkenes are formed directly from the surface methoxy groups, and at low concentrations can escape from the zeolite without oligomerisation, *i.e.* the oligomer is not formed directly from the methoxy groups but via alkenes.

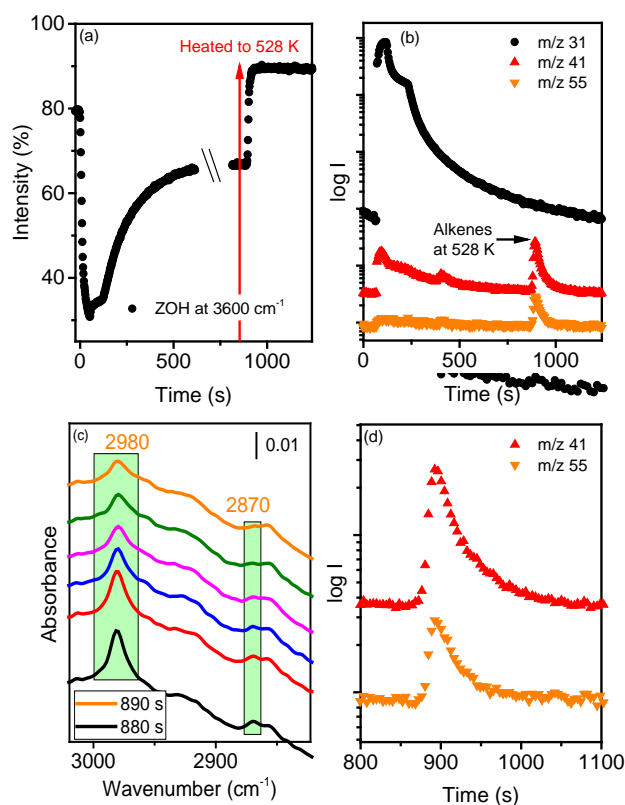


**Figure 4.** (a) ν(OH) intensity relative to initial fresh crystal versus time following injection of the second of two pulses of methanol over a ZSM-5 crystal at 523 K. Arrow marks the point at which the temperature was raised to 528 K. (b) Corresponding MS traces (m/z = 31 measures methanol (with a contribution from fragmentation of dimethylether); m/z = 41, propene (with a contribution from fragmentation of dimethylether), m/z = 55, butene). (c) Spectra measured at 2 s intervals in the ν(CH) region at the point where the ν(OH) intensity increases. (d) MS traces for propene (m/z = 41) and butene (m/z = 55) during the time interval where the ν(OH) intensity increases.

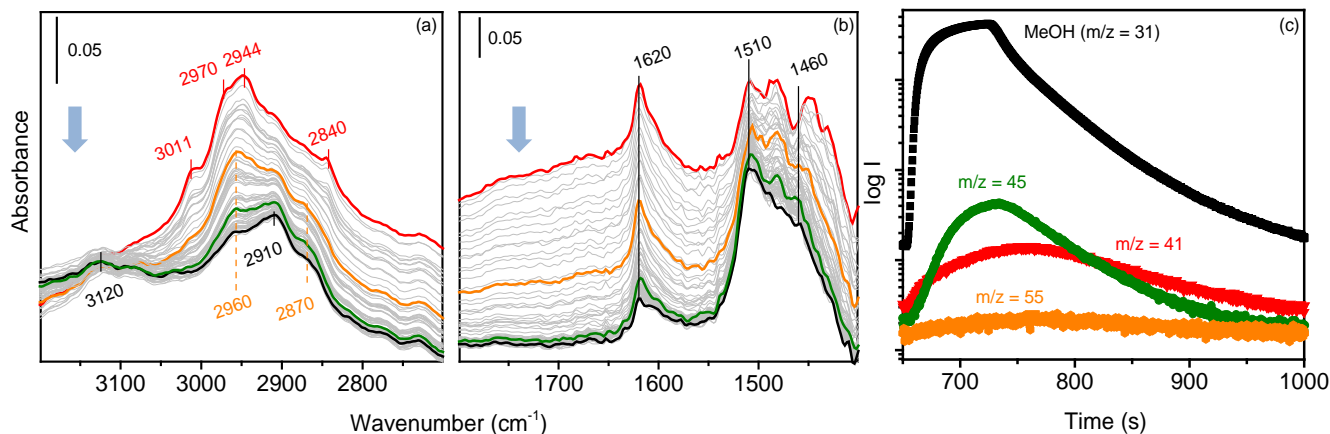


**Figure 5.** (a) Infrared spectra measured at 2 s intervals in (a) the v(CH) and (b) the v(C-C) regions following injection of a third 8  $\mu$ L pulse of methanol over an HZSM-5 crystal at 573 K 650 s after the first pulse shown in Fig. 1. Highlighted spectra in red, orange, green and black at 48, 76, 128 and 186 s after the injection. (c) MS traces during the third pulse (time axis is from the first pulse).  $m/z = 31$  measures methanol,  $m/z = 45$  measures DME,  $m/z = 41$  measures propene (with a contribution from DME fragmentation),  $m/z = 55$  measures butene.

The presence of a second hydrocarbon species showing bands at 3120, 2910, 1510 and 1460  $\text{cm}^{-1}$ , was revealed in the propene-pulse experiment after the decay of the oligomer bands (black trace in Fig. 3a). This hydrocarbon species is also evident in spectra recorded when multiple pulses of methanol were injected into an HZSM-5 crystal at 573 K. Fig. 5 shows, for example, spectra measured after injection of three successive 8  $\mu$ L pulses of methanol each  $\sim 300$  s apart. The spectra measured at the leading edge of the third methanol pulse in Fig. 5 are dominated by the bands of hydrogen bonded dimethylether (red trace), but as these are lost the oligomer species becomes evident (orange trace). Gradual loss of the oligomer bands reveals the second species generated from propene, which dominates the spectrum 186 s after injection of the third pulse (black trace). Also evident in the second and third pulses was an additional band at 1620  $\text{cm}^{-1}$  characteristic of methylated aromatics which was not seen in the first methanol pulse at 573 K or in the propene experiment at 523 K.

The second species generated from propene and formed in the second and third methanol pulses exhibiting bands at 3120, 2910, 1510 and 1460  $\text{cm}^{-1}$  is identified as the 1,3-dimethylcyclopentenyl cation (DMCP). The infrared spectrum of the DMCP cation in the gas phase is known.<sup>35</sup> The frequencies and relative intensities of the bands seen here with propene and methanol agree well with those reported for the gas phase species. The same species was generated by reacting dimethylether over crystals of HZSM-5; the frequencies and relative intensities of the DMCP bands are found to be the same in different sized crystals and at different reaction temperatures, whether generated from ethene, methanol, dimethylether, ethene or propene. Furthermore, the expected frequency shifts are seen when DMCP is formed from methanol- $d_4$  (see Fig. S11 and Table S2).

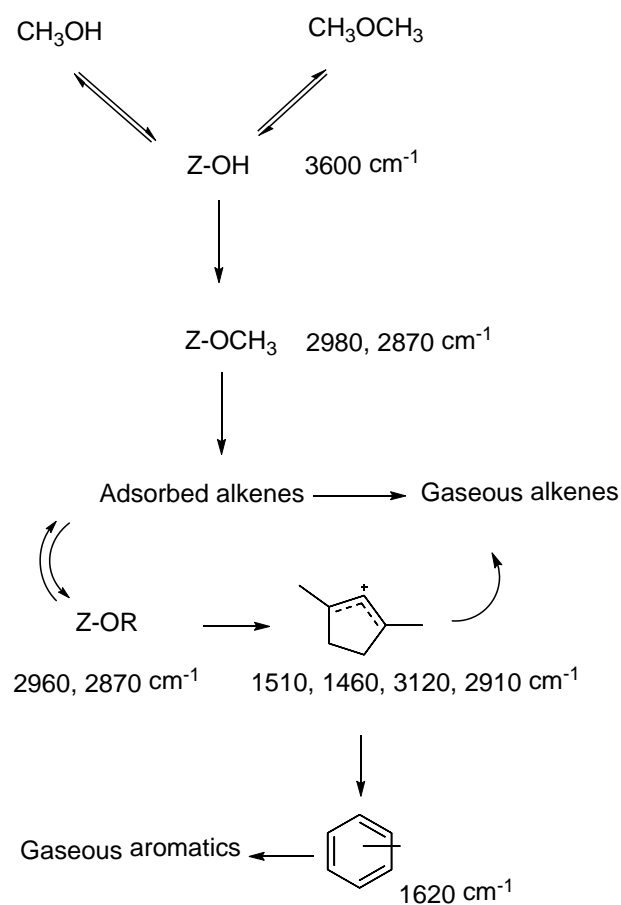
The importance of DMCP in MTH catalysis was first demonstrated in pulse-quench NMR experiments by Haw *et al.* who showed that the DMCP cation was generated in less than 8 seconds after injection of dimethylether into HZSM-5 at

573 K, and its appearance in the NMR spectrum correlated with the first formation of alkene products in the gas phase.<sup>36</sup> The same cation was generated when HZSM-5 was exposed to ethene at 623 K, and alkene products were generated on its decomposition. At lower temperatures, long chain oligomer species were formed from ethene. More recent NMR experiments have also identified cyclopentenyl cations as well as many other related cyclic cations as important components of the hydrocarbon pool in HZSM-5,<sup>5,6,37,38</sup> but according to Haw *et al.* the 1,3-dimethylcyclopentenyl species is the first one formed (and an explanation for its particular stability in ZSM-5 has been proposed<sup>39</sup>).

Theoretical calculations suggest that the formation of cyclic hydrocarbons from ethene and propene occurs via oligomeric species and that 5-ring formation precedes 6-ring formation.<sup>40</sup> As pointed out by Haw *et al.*, stoichiometry demands that formation of DMCP cations from oligomer requires concomitant formation of alkanes, *e.g.*  $\text{C}_9\text{H}_{19}\text{OZ} \rightarrow \text{C}_7\text{H}_{11}\text{OZ} + 2 \text{CH}_4$ . It is possible that the methane commonly reported as an initial product of methanol conversion over ZSM-5<sup>5,6</sup> is formed during the cyclisation step rather than through hydrogen abstraction from methanol by surface methoxy groups. Once DMCP is present in the zeolite it may undergo methylation and skeletal rearrangement to form toluene or other methylated aromatic products through chemistry which has been well described in the literature.<sup>5,6</sup> The weak 1620  $\text{cm}^{-1}$  band seen in the second and third methanol pulses is assigned to toluene or related aromatic species. At higher reaction temperatures and in smaller crystals this band has higher relative intensities, consistent with enhanced yields of methylaromatic products detected in the MS analysis (see Fig. S12). A relationship between the 1620  $\text{cm}^{-1}$  band and aromatic product yields was also seen when HZSM-5 crystals were exposed to a continuous flow of dimethylether at higher temperatures (Fig. S13).

Scheme 1 summarises the species detected in these infrared experiments along with the infrared frequencies assigned to them. The crucial initiating step in carbon-carbon bond for-

mation from methanol is the deprotonation of initially formed surface methoxy groups, which leads to alkene formation via carbene-like species.



**Scheme 1:** Reaction pathways and species identified spectroscopically in this work.

The fact that alkenes are formed only after adsorbed dimethylether is lost suggests that this chemistry does not involve reaction of the surface methoxy groups with adsorbed dimethylether, as previously proposed, but rather condensation of adjacent methoxy groups. The infrared spectra measured here show no evidence for formation of carboxylate groups expected from carbonylation of surface methoxy groups.<sup>15,17,18</sup> Fig. S15 shows spectra measured from methylacetate injected into HZSM-5 crystals at various temperatures, demonstrating the sensitivity of the technique to the presence of surface carboxylate species. We therefore believe that under the reaction conditions employed here a mechanism for direct carbon-carbon bond formation involving formaldehyde<sup>14,15,41,42</sup> or methylacetate<sup>17,18</sup> is not occurring. Once alkenes are formed, they may escape the zeolite or oligomerise. The resulting oligomer can crack to provide an additional source of alkenes or cyclise to form DMCP. The oligomer and the DMCP can be regarded as the first components of the hydrocarbon pool, and as suggested by Haw *et al.*<sup>36</sup> both act as a more efficient indirect source of alkenes (and ultimately methylaromatics) than the direct process seen in the initial stages of the reaction.

Detailed spectra and MS analyses from crystals of different size and at different reaction temperatures will be reported elsewhere.<sup>25</sup> The data presented here clearly illustrate the rapid time resolution achievable with synchrotron infrared microspectroscopy applied to single crystal zeolite catalysis, and we suggest that this technique should be readily applicable to many other types of zeolite-catalysed reactions.

## ASSOCIATED CONTENT

Supporting Information.

Synthesis and characterisation of HZSM-5 Crystals, Microreactor catalytic data, experimental procedures for synchrotron microspectroscopy measurements, supplementary infrared spectra and MS data.

The research data supporting this publication can be accessed at <https://doi.org/10.17630/d0e5a924-8850-4fe4-a56f-b00c7472f25a>.

## AUTHOR INFORMATION

Corresponding Author

\* E-mail: r.howe@abdn.ac.uk

Funding Sources

Engineering and Physical Sciences Research Council (EPSRC)

## ACKNOWLEDGMENTS

IBM and PAW would like to thank the EPSRC and CRITICAT Centre for Doctoral Training for Financial Support [PhD studentship to IBM, and supplementary equipment grant EP/L016419/1]. The UK Catalysis Hub is thanked for resources and support provided via membership of the UK Catalysis Hub Consortium and funded by EPSRC (grants EP/I038748/1, EP/I019693/1, EP/K014706/1, EP/K014668/1, EP/K014854/1, EP/K014714/1 and EP/M013219/1). We thank the Diamond Light Source for provision of beam time and support facilities at the MIRIAM beamline B22 (Experiments SM13725-1, SM16257-1, SM18680-1, SM20906-1).

## REFERENCES

- (1) Chang, C.D. Hydrocarbons from Methanol. *Catal. Rev. Sci. Eng.* **1983**, 25, 1-118.
- (2) Koempel, H.; Liebner, W. Lurgi's Methanol-to-Propene *Proc. 8<sup>th</sup> Nat. Gas Conv. Symp. Natal, Brazil*, **2007**, 261-281.
- (3) Jasper, S.; El-Halwagi, M.M. A Techno-Economic Comparison between Two Methanol-to-propene Processes. *Processes* **2015**, 3, 684-698.
- (4) Tian, P.; Wei, Y.; Ye, M.; Liu, Z. Methanol to Olefins (MTO): from Fundamentals to Commercialization. *ACS Catalysis* **2015**, 5, 1922-1938.
- (5) Olsbye U.; Svelle S.; Lillerud K. P.; Wei Z. H.; Chen Y. Y.; Li J. F.; Wang, J.G.; Fan, W. B. The Formation and Degradation of Active Species during Methanol Conversion Over Protonated Zeotype Catalysts. *Chem. Soc. Rev.* **2015**, 44, 7155-7176.

- (6) Yarulina, I.; Chowdhury, A.D.; Meirer, F.; Weckhuysen, B.M.; Gascon J. Recent Trends and Fundamental Insights into the Methanol-to-hydrocarbons Process. *Nature Catalysis* **2018**, 1, 398-411.
- (7) Ono, Y.; Mori, T. Mechanism of Methanol Conversion into Hydrocarbons over ZSM-5 Zeolite. *J. Chem. Soc., Faraday Trans. 1* **1981**, 77, 2209-2221.
- (8) Forester, T. R.; Wong, S. T.; Howe, R. F. In-situ FTIR of Methylating Species in ZSM-5. *Chem. Commun.* **1986**, 1611-1613.
- (9) Forester, T. R.; Howe, R.F. In-situ Studies of Methanol and Dimethylether in ZSM-5. *J. Am. Chem. Soc.* **1987**, 5076-5080.
- (10) O'Malley, A. J.; Parker, S. F.; Chutia A.; Farrow, M. R.; Silverwood, I.P.; Garcia-Sakai, V.; Catlow, C. R. A. Room Temperature Methoxylation in Zeolites: Insight Into a Key Step of the Methanol-to-hydrocarbons Process. *Chem. Commun.* **2016**, 2, 2897-2900.
- (11) Matam, S. K.; Howe, R. F., Thetford, A.; Catlow, C. R. A. Room Temperature Methoxylation in Zeolite H-ZSM-5: an *Operando* DRIFTS/Mass Spectrometric Study. *Chem. Commun.* **2018**, 4, 12875-12878.
- (12) Wang, W.; Seiler, M.; Hunger, M. Role of Surface Methoxy Species in the Conversion of Methanol to Dimethylether on Acidic Zeolites Investigated by *in-situ* Stopped Flow MAS NMR Spectroscopy. *J. Phys. Chem. B* **2001**, 105, 12553-12558.
- (13) Olah, G.A.; Doggweiler, H.; Felberg, J.D.; Frohlich, S.; Grdina, M.J.; Karpeles, R.; Keumi, T.; Inaba, S.; Ip, W.M.; Lammertsma, K.; Onium Ylide Chemistry. 1. Bifunctional Acid-base-catalyzed Conversion of Heterosubstituted Methanes into Ethylene and Derived Hydrocarbons. The Onium Ylide Mechanism of the C1 → C2 Conversion. *J. Am. Chem. Soc.* **1984**, 106, 2143-2149.
- (14) Hutchings, G.J.; Gottschalk, F.; Hall, M. V. M.; Hunter, R. Hydrocarbon Formation from Methylating Agents over the Zeolite Catalyst ZSM-5. *J. Chem. Soc. Farad. Trans.* **1987**, 83, 571-583.
- (15) Liu, Y.; Kirchberger, F. M.; Muller, S.; Eder, M.; Tonigold M.; Sanchez-Sanchez, M.; Lercher J. A. Critical Role of Formaldehyde During Methanol Conversion to Hydrocarbons. *Nature Commun.* **2019**, doi.org/10.1038/s41467-019-09449-7.
- (16) Li, J.; Wei, Z.; Chen, Y.; Jing, B.; He, Y.; Dong, M.; Jiao, H.; Li, X.; Qin, Z.; Wang, J.; Fan, W. A Route to Form Initial Hydrocarbon Pool Species in Methanol Conversion to Olefins over Zeolites. *J. Catal.* **2014**, 317, 277-283.
- (17) Liu, Y.; Muller, S.; Berger, D.; Jelic, J.; Reuter, K.; Tanigold, M.; Sanchez-Sanchez, M.; Lercher, J.A. Formation Mechanism of the First Carbon-carbon Bond and the First Olefin in the Methanol Conversion into Hydrocarbons. *Angew. Chem. Int. Ed.* **2016**, 55, 5723-5726.
- (18) Chowdhury, A.,D.; Houben, K.; Whiting, G.,T.; Mokhtar, M.; Asiri, A.M.; Al-Thabaiti, S.,A.; Basahel, S.,N.; Baldus, M.; Weckhuysen, B.M. Initial Carbon-carbon Bond Formation during the Early Stages of the Methanol to Olefins Process Proven by Zeolite Trapped Acetate and Methylacetate. *Angew. Chem. Int. Ed.* **2016**, 55, 5723-5726.
- (19) Yamazaki, H.; Shima, H.; Imai, H.; Yokoi, T.; Tatsumi, T.; Kondo, J.N. Direct Production of Propene from Methoxy Species and Dimethylether Over H-ZSM-5. *J. Phys. Chem. C* **2012**, 16, 24091-24097.
- (20) Van Wullen, L.; Koller, H.; Kalwer, M. Solid State Double Resonance Strategies for the Structural Characterization of Adsorbate Complexes involved in the MTG Process. *Phys. Chem. Chem. Phys.* **2002**, 4, 1665-1674.
- (21) Wu, X.; Xu, S.; Wei, Y.; Zhang, W.; Huang, J.; Xu, S.; He, Y.; Lin, S.; Sun, T.; Liu, Z. Evolution of C-C Bond Formation in the Methanol-to-olefins Process: from Direct Coupling to Autocatalysis. *ACS Catalysis* **2018**, 8, 7356-7361.
- (22) Stavitski, E.; Kox, M. H. F.; Swart, I.; de Groot, F. M. F.; Weckhuysen, B.M. *In-situ* Synchrotron-based IR Microspectroscopy to Study Catalytic Reactions in Zeolite Crystals. *Angew. Chem. Int. Ed.* **2008**, 47, 3543-354.
- (23) Stavitski, E.; Weckhuysen, B.M. Infrared and Raman Imaging of Heterogeneous Catalysts. *Chem. Soc. Rev.* **2010**, 39, 4615-4625.
- (24) Meirer, F.; Weckhuysen, B.M. Spatial and Temporal Exploration of Heterogeneous Catalysts with Synchrotron Radiation. *Nature Rev. Materials* **2018**, 3, 324-340.
- (25) Minova, I.B.; Matam S.K.; Greenaway A.; Suwardiyanto A.; Catlow C.R.A.; Frogley M.D.; Cinque G.; Wright P.A.; Howe R.F. Synchrotron Infrared Microspectroscopic Studies of Methanol Conversion over Individual Crystals of ZSM-5: Effects of Crystal Size, *in preparation*.
- (26) Zecchina, A.; Bordiga, S.; Spoto, G.; Scarano, D.; Spono, G.; Geobaldo, F. IR Spectroscopy of Neutral and Ionic Hydrogen Bonded Complexes from Interaction of CH<sub>3</sub>OH, C<sub>2</sub>H<sub>5</sub>OH, (CH<sub>3</sub>)<sub>2</sub>O, (C<sub>2</sub>H<sub>5</sub>)<sub>2</sub>O and C<sub>4</sub>H<sub>8</sub>O with H-Y, H-ZSM-5 and H-mordenite: Comparison with Analogous Adducts Formed on the H-Nafion Supercritical Membrane. *J. Chem. Soc. Farad. Trans.* **1996**, 92, 4863-4875.
- (27) Bordiga, S.; Lamberti, C.; Bonino, F.; Travert, A.; Thibault-Starzyk, F. Probing Zeolites by Vibrational Spectroscopy. *Chem. Soc. Rev.* **2015**, 44, 7262-7341.
- (28) Kondo, J.N.; Yamazaki, H.; Yokoi, T.; Tatsumi, T. Mechanisms of Reactions of Methoxy Species with Benzene and Cyclohexane Over H-ZSM-5 Zeolites. *Catal. Sci. Tech.* **2015**, 5, 3598-3602.
- (29) Yamagishi, K.; Namba, S.; Yashima, T. Defect Sites in Highly Siliceous HZSM-5 Zeolites: a Study Performed by Aluminations and IR Spectroscopy. *J. Phys. Chem.* **1991**, 91, 872-877.
- (30) Falk, M.; Whalley, E. Infrared Spectra of Methanol and Deuterated Methanols in Gas, Liquid, and Solid Phases. *J. Chem. Phys.* **1961**, 34, 1554-1568.
- (31) Yamazaki, H.; Shima, H.; Imai, H.; Yokoi, T.; Tatsumi, T.N.; Kondo, J.N. Evidence for a "Carbene-like" Intermediate during the Reaction of Methoxy Species with Light Alkenes on HZSM-5. *Angew. Chem. Int. Ed.* **2011**, 50, 1853-1856.
- (32) Kiricsi, I.; Forster, H.; Tasi, G.; Nagy, J. B. Generation, Characterisation and Transformations of Unsaturated Carbenium Ions in Zeolites. *Chem. Rev.* **1999**, 99, 2085-2114.
- (33) Spoto, G.; Bordiga, S.; Ricciardi, G.; Scarano, D.; Zecchina, A.; Borello, E. IR Study of Ethene and Propene Oligomerization on H-ZSM-5: Hydrogen-bonded Precursor Formation, Initiation and Propagation Mechanisms and Structure of the Entrapped Oligomers. *Faraday Trans.* **1994**, 90, 2827-2835.
- (34) Milnar, A.; Zimmerman, P. M.; Celik, F. E.; Gordon, M. H.; Bell, A. T.; Effects of Bronsted Acid Proximity on the Oligomerization of Propene in HMF1. *J. Catal.* **2012**, 288, 65-73.
- (35) Mosley, J. D.; Young, J. W.; Agarwal, J.; Schaefer, H. F.; Schleyer, P. R.; Duncan, M. A. Structural Isomerization of the Gas-phase 2-norbornyl Cation Revealed with Infrared Spectroscopy and Computational Chemistry. *Angew. Chem. Int. Ed.* **2014**, 53, 5888-5891.
- (36) Haw, J. F.; Nicholas, J. B.; Song, W.; Deng, F.; Wang, Z.; Xu, T.; Heneghan, C. Roles for Cyclopentenyl Cations in the Synthesis of Hydrocarbons from Methanol on Zeolite Catalyst H-ZSM-5. *J. Am. Chem. Soc.* **2000**, 122, 4763-4775.
- (37) Xiao, D.; Xu, S.; Han, X.; Bao, X.; Liu, Z.; Blanc, F. Direct Structural Identification of Carbenium Ions and Investigation of Host-Guest Interactions in the Methanol to Olefins Reaction Obtained by Multi-nuclear NMR Correlations. *Chem. Sci.* **2017**, 8, 8309-8314.
- (38) Wang, C.; Chu, Y.; Zheng, A.; Xu, J.; Wang, Q.; Gao, P.; Qi, G.; Gong, Y.; Deng, F. New Insight into the Hydrocarbon-pool Chemistry of the Methanol-to-olefins Conversion over Zeolite HZSM-5 from GCMS, Solid-state NMR Spectroscopy, and DFT Calculations. *Chem. Eur. J.* **2014**, 20, 12432-12443.
- (39) Song, W.; Nicholas, J. B.; Haw, J. F. Acid-base Chemistry of a Carbenium Ion in a Zeolite under Equilibrium Conditions: Verification of a Theoretical Explanation of Carbenium Ion Stability. *J. Am. Chem. Soc.* **2001**, 123, 121-129.
- (40) Vandichel, M.; Lesthaeghe, D.; van der Mynsbrugge, J.; Waroquier, M.; van Spreybroeck, V. Assembly of Cyclic Hydrocarbons from Ethene and Propene in Acid Zeolite Catalysis to Produce Active Catalytic Sites for MTO Conversion. *J. Catal.* **2010**, 271, 67-78.

(41) Martinez-Espin, J. S.; De Wispelaere K.; Janssens, T. V. W.; Svelle, S.; Lillerud, K. P.; Beato, P.; Van Speybroeck, V.; Olsbye, U. Hydrogen Transfer versus Methylation: On the Genesis of Aromatics Formation in the Methanol-To-Hydrocarbons Reaction over H-ZSM-5. *ACS Catalysis* **2017**, *7*, 5773-5780.

(42) Arora, S. S.; Bhan, A. The Critical Role of Methanol Pressure in Controlling its Transfer Dehydrogenation and the Corresponding Effect on Propylene to Ethylene Ratio during Methanol-to-Hydrocarbons Catalysis on H-ZSM-5. *J. Catal.* **2017**, *356*, 300-306.

### For Table of Contents Only

